

## Effect of Salt and pH on the Reductive Half-Reaction of *Mycobacterium tuberculosis* FprA with NADPH<sup>†</sup>

Andrea Pennati,<sup>‡</sup> Giuliana Zanetti,<sup>‡</sup> Alessandro Aliverti,<sup>\*,‡</sup> and Giovanni Gadda<sup>\*,§</sup>

Dipartimento di Scienze Biomolecolari e Biotecnologie, Università degli Studi di Milano, via Celoria 26, 20133 Milano, Italy, and Departments of Chemistry and Biology and The Center for Biotechnology and Drug Design, Georgia State University, Atlanta, Georgia 30302

Received November 12, 2007; Revised Manuscript Received January 21, 2008

**ABSTRACT:** Despite a number of studies, the formation of the Michaelis complexes between ferredoxin-NADP<sup>+</sup> reductases and NADP(H) eluded detailed investigations by rapid kinetic techniques because of their high formation rates. Moreover, the reversible nature of the reaction of hydride ion transfer between these enzymes and NADPH prevented the obtainment of reliable estimates of the rate constant of the hydride transfer step. Here we show that by working at a high salt concentration, the mechanism of the reaction with NADPH of FprA, a *Mycobacterium tuberculosis* homologue of adrenodoxin reductase, is greatly simplified, making it amenable to investigation by rapid reaction techniques. The approach presented herein allowed for the first time the observation of the formation of the Michaelis complex between an adrenodoxin reductase-like enzyme and NADPH, and the determination of the related rate constants for association and dissociation. Furthermore, the rate constant for the reaction of hydride ion transfer between NADPH and FAD could be unambiguously assessed. It is proposed that the approach described should be applicable to other ferredoxin reductase enzymes, providing a valuable experimental tool for the study of their kinetic properties.

A number of flavin-dependent enzymes, including plant and bacterial ferredoxin-NADP<sup>+</sup> oxidoreductases (1–4), adrenodoxin reductase (5, 6), microsomal cytochrome P450 reductase (7, 8), and nitric oxide synthase (9), are known to participate in reversible hydride ion transfer reactions in which the donor of the hydride ion is the reduced form of nicotinamide adenine dinucleotide phosphate (NADPH).<sup>1</sup> These reactions are amenable to investigation by using stopped-flow spectrophotometric approaches, in which the reduction of the enzyme-bound flavin is monitored directly at 450 nm when the oxidized form of enzyme is mixed anaerobically with NADPH. However, a number of studies have pointed out severe limitations of the rapid kinetic approach when it is applied to flavin-dependent enzymes that utilize NADPH for reducing

power (10), thereby limiting the understanding of these biochemically important enzymes. Usually, the formation of the Michaelis complex that precedes the hydride transfer reaction is too fast to be studied by rapid mixing techniques (11, 12). Moreover, due to the reversible nature of the reaction and the tight binding of the pyridine nucleotides to the enzyme (11, 12), the apparent rate of the hydride transfer process decreases to a limiting value with an increase in the concentration of NADPH, rather than showing saturation kinetics (2, 5, 10–12).

Our group recently cloned and expressed the gene encoding FprA from *Mycobacterium tuberculosis* strain H37Rv and characterized the purified enzyme with respect to its biochemical, kinetic, and structural properties (12–14). The enzyme is a monomer of 50 kDa that catalyzes the transfer of a hydride equivalent from NADPH to a yet-unidentified electron acceptor via tightly, but not covalently, bound FAD (13). NADH can also be used as a source of reducing power in catalysis, although with a  $K_m$  value that is ~100-fold larger than that for NADPH (13). On the basis of the amino acid sequences, FprA is homologous to mammalian adrenodoxin reductase (13, 14), for which adrenodoxin, a two-Fe ferredoxin, acts as the electron acceptor (15, 16). However, since no genes encoding two-Fe ferredoxins have been identified in the genome of *M. tuberculosis* (17), the nature of the physiological electron acceptor of FprA remains elusive. In this context, evidence that this role could be fulfilled by both seven-Fe and three-Fe ferredoxins has been provided (18). The X-ray crystallographic structures of FprA with either NADP<sup>+</sup> or NADPH have been recently reported at resolutions of 1.25 Å or better (14), showing an overall structure that is very similar to that of bovine adrenodoxin re-

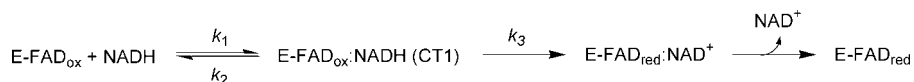
<sup>†</sup> This work was supported in part by a NSF CAREER Award (MCB-0545712) and a grant from the American Chemical Society Petroleum Research Fund (47636-AC4) to G.G. and by grants from Fondazione Cariplo, Milano, Italy, and from Ministero dell'Università e della Ricerca of Italy (PRIN 2005) to G.Z. A.P. is grateful for a Wood-Whelan Research Fellowship to support his visit to Georgia State University.

\* To whom correspondence should be addressed. G.G.: Department of Chemistry, Georgia State University, P.O. Box 4098, Atlanta, GA 30302-4098; phone, (404) 413-5537; fax, (404) 413-5505; e-mail, ggadda@gsu.edu. A.A.: Dipartimento di Scienze Biomolecolari e Biotecnologie, via Celoria 26, 20133 Milano, Italy; fax, +39 02 50314895; e-mail, alessandro.aliverti@unimi.it.

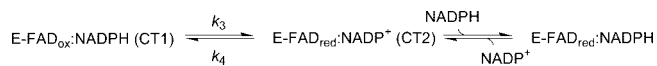
<sup>‡</sup> Università degli Studi di Milano.

<sup>§</sup> Georgia State University.

<sup>1</sup> Abbreviations: NADPH, reduced form of nicotinamide adenine dinucleotide phosphate; NADH, reduced form of nicotinamide adenine dinucleotide; CT1, charge transfer complex of enzyme-bound FAD and NADPH; CT2, charge transfer complex of enzyme-bound reduced FAD and NADP<sup>+</sup>; NADPO, 3-carboxamide-4-pyridone adenine dinucleotide phosphate.

Scheme 1: Minimal Kinetic Mechanism for the Reductive Half-Reaction of FprA with NADH<sup>a</sup>

<sup>a</sup> E-FAD<sub>ox</sub> and E-FAD<sub>red</sub> represent oxidized and reduced FprA, respectively.

Scheme 2: Minimal Kinetic Mechanism for the Reductive Half-Reaction of FprA with NADPH<sup>a</sup>

<sup>a</sup> E-FAD<sub>ox</sub> and E-FAD<sub>red</sub> represent oxidized and reduced FprA, respectively.

ductase (19, 20). The atomic-resolution structure (1.05 Å) of FprA in complex with NADP<sup>+</sup> revealed a novel covalently modified form of the pyridine nucleotide, which was identified using mass spectrometric analysis as its 4-oxo derivative, named NADPO (14, 21). Interestingly, in the atomic-resolution structure of the FprA–NADPO complex, the positively charged side chains of Arg-199 and Arg-200 are ≤2.9 Å from the 2'-phosphoryl oxygens of NADPO, suggesting that electrostatic interactions may play an important role for the binding of NADPH (14, 22, 23). The reductive half-reaction of FprA with either NADPH or NADH as the substrate has been investigated using stopped-flow techniques at pH 7 (12). With NADH as the source of hydride ion, both the formation of the E-FAD<sub>ox</sub>–NADH Michaelis complex, which results in a charge transfer species (CT1) with an absorbance band in the 530 nm region, and the subsequent reaction of hydride ion transfer to the enzyme-bound flavin are kinetically detectable (Scheme 1) (12). Accordingly, a second-order rate constant for the association of NADH with the enzyme (*k*<sub>1</sub>) to form the CT1 species of ~140 mM<sup>-1</sup> s<sup>-1</sup> and a limiting first-order rate constant (*k*<sub>lim</sub>) for the irreversible reaction of hydride ion transfer to the enzyme-bound flavin of ~18 s<sup>-1</sup> were determined with NADH (12). In contrast, with NADPH as the reductant, formation of the CT1 species was too fast to be observed (12). Moreover, the observed rates for the hydride ion transfer reaction decreased with increasing concentrations of NADPH to a limiting value of ~18 s<sup>-1</sup> (12), consistent with a minimal kinetic mechanism in which NADPH and NADP<sup>+</sup> are in rapid equilibrium with the reduced form of the enzyme (Scheme 2). In this context, the lack of saturation kinetics with NADPH prevents the possible dissection of the limiting rate constant (*k*<sub>lim</sub>) determined at high concentrations of NADPH in its forward and reverse components by using kinetic approaches (12, 24). Thus, only limited mechanistic information is available for the reaction of hydride ion transfer catalyzed by FprA with the physiological substrate NADPH.

In this study, we have investigated the effects of salt and pH on the reductive half-reaction of FprA with NADPH, with the goal of simplifying the minimal kinetic mechanism that describes the reaction of the enzyme with this pyridine nucleotide, and render the reaction amenable to investigation by using rapid reaction techniques. The kinetic data presented herein allowed the first direct observation of the formation of the Michaelis complex between FprA and NADPH and an unambiguous determination of the second-order rate constants for formation

of the CT1 species with NADPH. This study, therefore, improves our understanding of the mechanism of hydride ion transfer in the adrenodoxin reductase-like FprA, and to a broader extent, it provides simple tools for further investigating similar chemical reactions that are catalyzed by other flavoenzymes with medical and biological relevance, such as cytochrome P450 reductase, nitric oxide synthase, adrenodoxin reductase, and plant-type ferredoxin-NADP<sup>+</sup> oxidoreductase.

## EXPERIMENTAL PROCEDURES

**Materials.** Recombinant *M. tuberculosis* FprA was purified from *Escherichia coli* cells as described previously (12). The N-terminal peptide extension containing a poly-His sequence was not cleaved off, since it does not affect the kinetic properties of the enzyme (12). All reagents were of the highest purity commercially available.

**Methods.** All stopped-flow studies of the reductive half-reaction catalyzed by FprA were performed at 25 °C using a Hi-Tech Scientific SF-61 DX2 stopped-flow spectrophotometer under anaerobic conditions. FprA aliquots were gel filtered through a PD-10 column (GE Healthcare) against 50 mM Hepes-NaOH (pH 7) or 50 mM glycine-NaOH (pH 10), each containing 10% glycerol and variable concentrations of NaCl ranging from 0 to 3 M. The concentration of the enzyme was adjusted to ~50 μM, and the solution was made anaerobic in a tonometer by repeated cycles of evacuation and flushing with oxygen-free argon (pretreated with an oxygen scrubbing cartridge, Agilent, Palo Alto, CA). Subsequently, the anaerobic enzyme solution was mounted onto the stopped-flow instrument, which had been subjected to an overnight incubation with an oxygen scrubbing system containing 5 mM sodium dithionite. NADPH solutions were prepared fresh in the same buffer system used for FprA at concentrations ranging from 0.15 to 3 mM and were degassed by being flushed with oxygen-free argon for at least 20 min before being mounted onto the stopped-flow instrument. FprA was mixed anaerobically with an equal volume of NADPH in the stopped-flow spectrophotometer, and the changes in absorbance at 450, 530, or 700 nm were followed. Duplicate measurements differed typically by less than 5%. The dependence of the UV–visible absorbance spectrum of FprA on pH was determined in 20 mM sodium phosphate, 20 mM sodium pyrophosphate, and 10% glycerol, over the pH range from 6 to 12.5. The enzyme solution was freshly prepared by gel filtration through a PD-10 column equilibrated in the incubation buffer adjusted to pH 6 in the absence or presence of 2.5 M NaCl. The pH was carefully titrated with the addition of small volumes of 1 M NaOH into a 3 mL spectrophotometer cuvette thermostated at 15 °C. Spectral changes elicited by each base addition ensued very rapidly and were stable for minutes.

**Data Analysis.** Stopped-flow traces at individual wavelengths were fit to either eq 1, which describes a single-exponential process, or eq 2, which describes a double-

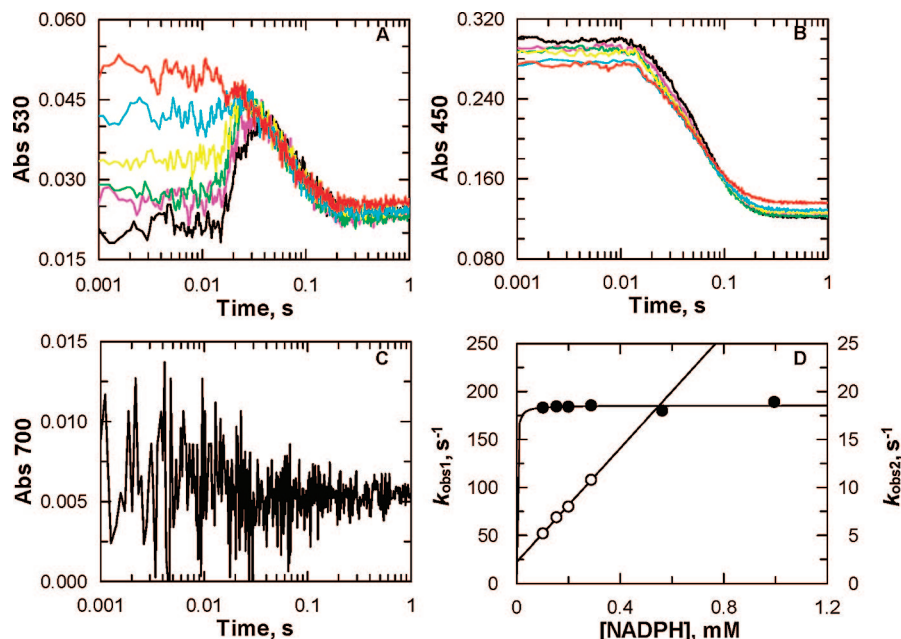


FIGURE 1: Anaerobic reduction of FprA with NADPH at pH 7 in the presence of 1 M NaCl. Reactions were carried out in a stopped-flow spectrophotometer with 0.1 (black), 0.15 (fuchsia), 0.2 (lime), 0.29 (yellow), 0.57 (aqua), and 1 mM NADPH (red), in the presence of 1 M NaCl in 50 mM Hepes-NaOH and 10% glycerol (pH 7) at 25 °C. The concentration of enzyme after mixing was 0.025 mM. Panels A and B show stopped-flow traces at 530 and 450 nm, respectively. Panel C shows a stopped-flow trace at 700 nm with 0.1 mM NADPH. Time indicated is after the end of flow, i.e., 2.2 ms. Panel D shows the observed rates  $k_{\text{obs1}}$  (○) and  $k_{\text{obs2}}$  (●) for flavin reduction determined at 450 nm as a function of the concentration of NADPH. Data for  $k_{\text{obs1}}$  and  $k_{\text{obs2}}$  were fit to eq 3 and 4, respectively.

exponential process, using KinetAsyst 3 (Hi-Tech Scientific) or GraFit 5 (Erythacus Software Ltd., Staines, U.K.).

$$A = B \exp(-k_{\text{obs}}t) + C \quad (1)$$

$$A = B_1 \exp(-k_{\text{obs1}}t) + B_2 \exp(-k_{\text{obs2}}t) + C \quad (2)$$

where  $A$  is the value of the absorbance at the specific wavelength of interest,  $k_{\text{obs}}$ ,  $k_{\text{obs1}}$ , and  $k_{\text{obs2}}$  are the apparent first-order rate constants for the observed phases of the reaction,  $B$ ,  $B_1$ , and  $B_2$  are the corresponding amplitudes for the change in absorbance associated with the phase of interest, and  $C$  is an offset value to account for a non-zero final absorbance value. The dependence of the observed rate constants on the concentration of NADPH was analyzed by fitting the data with either a straight line (eq 3) or a rectangular hyperbola (eq 4), as appropriate. When two phases were observed in the stopped-flow traces, the analysis allowed for the calculation of microscopic rate constants on the basis of eqs 3 and 4 (24).

$$k_{\text{obs1}} = k_1 [\text{NADPH}] + C \quad (3)$$

$$k_{\text{obs2}} = \frac{k_{\text{lim}} [\text{NADPH}]}{K_d + [\text{NADPH}]} \quad (4)$$

where  $k_{\text{obs1}}$  and  $k_{\text{obs2}}$  are the observed first-order rate constants for the fast and slow phases of the reaction, respectively,  $k_1$  is the second-order rate constant for the formation of the oxidized enzyme–NADPH Michaelis complex,  $C$  represents the y-intercept in a plot of  $k_{\text{obs1}}$  versus  $[\text{NADPH}]$ ,  $k_{\text{lim}}$  is the first-order rate constant for the reduction of the enzyme-bound flavin with saturated concentrations of NADPH, and  $K_d$  represents the thermodynamic equilibrium constant for the dissociation of the FprA<sub>ox</sub>–NADPH complex. When a single phase was observed in the stopped-flow traces,  $k_{\text{obs}}$  showed a hyperbolic dependence on the concentration of NADPH, allowing for the calculation of the values of  $k_{\text{lim}}$

and  $K_d$ , according to 4, but not that of  $k_1$ . Data for the pH dependencies of the absorbance spectra for FprA were fit to eq 5, which describes the dissociation of a single ionizable group. Here,  $Y$  is the absorbance at 386 nm at any pH value, and  $A$  and  $B$  represent its limiting values at low and high pH, respectively.

$$Y = \frac{A \times 10^{-\text{pH}} + B \times 10^{-\text{p}K_a}}{10^{-\text{pH}} + 10^{-\text{p}K_a}} \quad (5)$$

## RESULTS

**Anaerobic NADPH Reduction of FprA at pH 7 in the Presence of 1 M NaCl.** With the aim of finding conditions under which the affinity of FprA for NADP(H) was lowered, we studied the effect of salt on the reduction of FprA with NADPH. The enzyme was mixed anaerobically with varying concentrations of NADPH in a stopped-flow spectrophotometer in the presence of 1 M NaCl at pH 7 and 25 °C, and the resulting changes in the visible absorbance associated with the enzyme-bound flavin were monitored over time. At concentrations of NADPH up to 0.3 mM, the absorbance traces at 530 nm were markedly biphasic, with a rapid increase in intensity occurring within the first 30 ms of reaction, followed by a slow decrease in absorbance that was completed within 250 ms (Figure 1A). In agreement with a biphasic process for flavin reduction, the best fit of the absorbance traces at 530 nm was obtained with eq 2, which describes a double-exponential kinetic process for flavin reduction. The same equation gave the best fit for the traces at 450 nm (Figure 1B). At concentrations of NADPH above 0.3 mM, the fast phase was completed within the dead time of the stopped-flow instrument, i.e., approximately 2 ms, allowing for the observation of the slow phase only (Figure 1A). On the basis of the known spectroscopic properties of

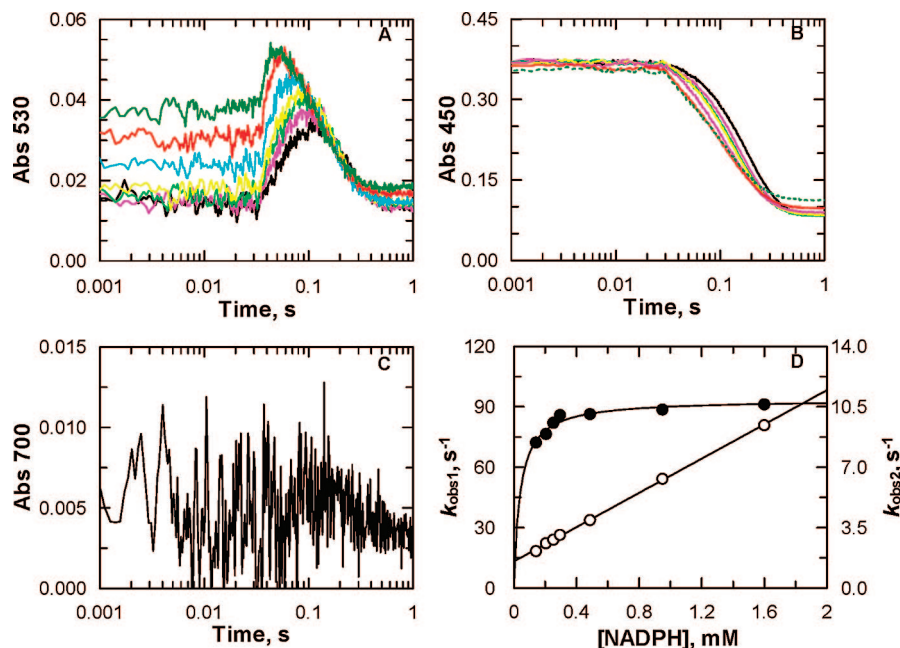


FIGURE 2: Anaerobic reduction of FprA with NADPH at pH 7 in the presence of 3 M NaCl. Reactions were carried out in a stopped-flow spectrophotometer with NADPH in the presence of 3 M NaCl in 50 mM Hepes-NaOH and 10% glycerol (pH 7) at 25 °C. Anaerobic FprA (final concentration of 0.03 mM) was mixed with anaerobic substrate: 0.15 (black), 0.2 (fuchsia), 0.25 (lime), 0.29 (yellow), 0.47 (aqua), 0.95 (red), and 1.6 mM (green). Panels A and B show stopped-flow traces at 530 and 450 nm, respectively. Panel C shows the stopped-flow trace at 700 nm with 0.15 mM NADPH. Time indicated is after the end of flow, i.e., 2.2 ms. Panel D shows the observed rates  $k_{\text{obs1}}$  (○) and  $k_{\text{obs2}}$  (●) for flavin reduction determined at 450 nm as a function of the concentration of NADPH. Data were fit to eqs 3 and 4, respectively.

FprA in different redox states or in complex with various ligands (12, 13), the increase in absorbance at 530 nm was assigned to the transient formation of a charge transfer complex species (CT1) between the oxidized enzyme and NADPH, which preceded the reduction of the enzyme-bound flavin via the hydride ion transfer reaction from NADPH to the flavin. As illustrated in the example of Figure 1C, there was no observable formation of a CT2 species between the reduced enzyme and  $\text{NADP}^+$ , consistent with rapid dissociation of the  $\text{NADP}^+$  product of the hydride transfer reaction from the reduced FprA enzyme. The observed rates for formation of the CT1 species ( $k_{\text{obs1}}$ ) were linearly dependent on the concentration of NADPH, yielding a y-intercept value of  $22.3 \pm 1.9 \text{ s}^{-1}$  and a slope of  $296 \pm 10 \text{ mM}^{-1} \text{ s}^{-1}$  (Figure 1D). Instead, the observed rates for flavin reduction ( $k_{\text{obs2}}$ ) were independent of the concentration of NADPH with an average value of  $18.5 \pm 0.2 \text{ s}^{-1}$ , suggesting that the enzyme was saturated with the substrate between 0.1 and 0.9 mM NADPH (Figure 1D).

**Effect of Increasing the NaCl Concentration above 1 M on Anaerobic Reduction of FprA with NADPH at pH 7.** The reduction of FprA with NADPH was further studied at concentrations of NaCl up to 3 M to evaluate whether the observed rates for flavin reduction ( $k_{\text{obs2}}$ ) showed any dependence on the concentration of NADPH.<sup>2</sup> Increasing the concentration of NaCl to 2 or 2.5 M yielded results that were qualitatively similar to those observed in the presence of 1 M NaCl, with observed rates for formation of the CT1 species ( $k_{\text{obs1}}$ ) being linearly dependent on the NADPH

concentration and observed rates for flavin reduction being independent of the concentration of substrate (Figure S1 of the Supporting Information). In contrast, in the presence of 3 M NaCl, the plot of  $k_{\text{obs2}}$  versus NADPH concentration showed hyperbolic saturation kinetics, yielding a limiting value for flavin reduction at a saturating concentration of NADPH of  $10.9 \pm 0.2 \text{ s}^{-1}$ , and an approximate  $K_d$  value<sup>3</sup> of  $\sim 40 \mu\text{M}$  (Figure 2). This represents the first instance in which the rate of flavin reduction of FprA with NADPH was shown to increase to a limiting value with increasing concentrations of substrate, as previously reported only with NADH as the hydride donor in the reaction (12). Remarkably, the slopes of the lines in the plots of  $k_{\text{obs1}}$  versus NADPH concentration decreased 10-fold with an increase in the concentration of NaCl from 1 to 3 M (Table 1), consistent with the rates of formation of the CT1 species being affected by the concentration of salt in solution. Instead, both the y-intercepts of the lines in the plots of  $k_{\text{obs1}}$  versus NADPH concentration and the limiting values for flavin reduction observed at a saturating concentration of NADPH ( $k_{\text{obs2}}$ ) decreased less than 2-fold with an increase in the concentration of NaCl (Table 1).

**Anaerobic NADPH Reduction of FprA at pH 10.** The reduction of FprA with NADPH in the presence of high concentrations of salt was also investigated at pH 10, with the objective of determining an accurate value for  $K_d$  of the FprA–NADPH complex. Since the interaction between FprA

<sup>2</sup> At concentrations of NaCl above 3 M, the viscosity of the solutions was too high to allow efficient mixing of the enzyme and substrate in the stopped-flow spectrophotometer, thereby preventing the acquisition of kinetic data at concentrations  $> 3 \text{ M}$  NaCl.

<sup>3</sup> The approximate  $K_d$  value is reported here because concentrations of NADPH that were lower than 0.1 mM could not be used in the stopped-flow spectrophotometer due to the FprA concentration being 0.025 mM, and the requirement that substrate concentration be greater than enzyme concentration to maintain pseudo-first-order conditions for the reaction of the enzyme with NADPH. Consequently, an accurate determination of the  $K_d$  value could not be carried out.

Table 1: Kinetic Rate Constants for Anaerobic Reduction of FprA with NADPH in the Presence of NaCl at pH 7<sup>a</sup>

[NaCl] (M)	$k_1^b$ (mM <sup>-1</sup> s <sup>-1</sup> )	$C^b$ (s <sup>-1</sup> )	$k_{lim}^b$ (s <sup>-1</sup> )	$k_2^c$ (s <sup>-1</sup> )	$K_d^d$ (μM)
0.1 <sup>e</sup>	nd <sup>f</sup>	nd <sup>f</sup>	18.0 ± 0.4	nd <sup>f</sup>	nd <sup>f</sup>
1	296 ± 10	22.3 ± 1.9	18.5 ± 0.2	3.8 ± 1.9	13 ± 6
2	149 ± 5.5	16.6 ± 2.0	12.6 ± 0.4	4.0 ± 2.0	27 ± 13
2.5	94.1 ± 2.3	13.0 ± 1.4	10.2 ± 0.2	2.8 ± 1.4	30 ± 15
3	42.5 ± 0.5	13.2 ± 0.4	10.9 ± 0.2	2.3 ± 0.4	54 ± 9

<sup>a</sup> Reactions were carried out in a stopped-flow spectrophotometer with NADPH in the presence of NaCl in 50 mM Hepes-NaOH and 10% glycerol (pH 7) at 25 °C. The observed rates  $k_{obs1}$  and  $k_{obs2}$  for flavin reduction monitored at 450 nm as a function of the concentration of NADPH were fit to eqs 3 and 4, respectively. <sup>b</sup>  $k_1$  and  $C$  are the values of the slope and y-intercept determined by fitting the data in a plot of  $k_{obs1}$  as a function of NADPH concentration to eq 3;  $k_{lim}$  is the limiting value for flavin reduction at a saturating concentration of NADPH determined by fitting the data in plot of  $k_{obs2}$  as a function of NADPH concentration to eq 4. <sup>c</sup>  $k_2$  values were calculated as described in the text by subtracting the  $k_{lim}$  values from the  $C$  values. <sup>d</sup>  $K_d$  values were calculated from  $k_2/k_1$  ratios. <sup>e</sup> Data are from ref 12. <sup>f</sup> Not observed.

and NADP(H) is mediated by several contacts involving ionizable groups of the protein (14), we hypothesized that a 3-unit increase in the pH of the reaction medium could weaken the affinity of the enzyme for NADPH. FprA was mixed anaerobically with the NADPH concentration ranging from 0.1 to 1.27 mM in a stopped-flow spectrophotometer in the presence of 2.5 M NaCl at pH 10 and 25 °C, and the reaction was monitored at 450 and 530 nm. As shown in Figure 3A, the reduction of the enzyme-bound flavin was monophasic at all concentrations of NADPH that were tested. Surprisingly, no increase in absorbance at 530 nm was observed during the time courses of enzyme reduction or within the dead time of the stopped-flow spectrophotometer, suggesting a lack of transient formation of the CT1 species between FprA and NADPH with 2.5 M NaCl at pH 10 (Figure 3A). A plot of the observed rates of flavin reduction as a function of the concentration of NADPH yielded a rectangular hyperbola (Figure 3B), allowing for the determination of an upper limiting value for  $k_{obs}$  of  $9.2 \pm 0.2$  s<sup>-1</sup> and a  $K_d$  value of  $90 \pm 10$  μM. As shown in the inset of Figure 3B, treatment of the kinetic data in double-reciprocal form yielded a straight line, consistent with FprA and NADPH binding in rapid equilibrium, and a negligible rate constant for the reverse of the hydride transfer reaction (24).

The reaction of FprA with NADPH at pH 10 was also studied in the absence of NaCl. As illustrated from the traces at 530 nm in the example of Figure S2 of the Supporting Information, a significant amount of the CT1 species was observed within the dead time of the stopped-flow spectrophotometer.<sup>4</sup> At all the concentrations of NADPH used, the kinetic data fit best to a single-exponential decay process at

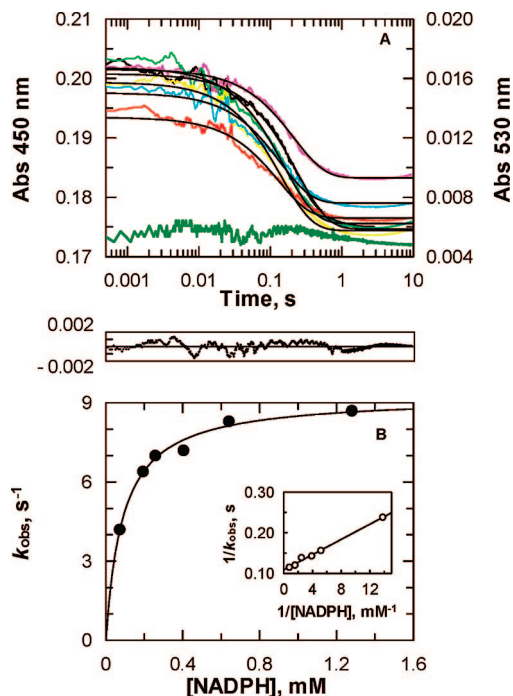


FIGURE 3: Anaerobic reduction of FprA with NADPH at pH 10 in the presence of 2.5 M NaCl. (A) Reactions were monitored at 450 nm in a stopped-flow spectrophotometer with 0.075 (black), 0.19 (fuchsia), 0.26 (lime), 0.40 (yellow), 0.6 (aqua), and 1.28 mM NADPH (red), in the presence of 2.5 M NaCl in 50 mM glycine-HCl and 10% glycerol (pH 10) at 25 °C. All the traces were fitted with eq 1. As a matter of example, the plot of the residuals for the trace at 0.075 mM NADPH is shown at the bottom of panel A. The green line represents the stopped-flow trace with 0.19 mM NADPH monitored at 530 nm. The concentration of enzyme after mixing was 0.025 mM. Time indicated is after the end of flow, i.e., 2.2 ms. Panel B shows the observed rates for flavin reduction determined at 450 nm as a function of the concentration of NADPH. Data were fit to eq 4. The inset shows a double-reciprocal plot of the observed rate of flavin reduction vs NADPH concentration.

both 450 and 530 nm, allowing for the determination of the concentration dependence of the observed rate of flavin reduction. As expected from previous results on the reduction of FprA with NADPH at pH 7 in the presence of 0.1 M NaCl (12), the  $k_{obs}$  values decreased to a limiting value with an increase in the concentration of NADPH (Figure S3 of the Supporting Information). Thus, irrespective of whether the pH is 7 or 10, a significant simplification of the reaction mechanism could be obtained only when concentrations of NaCl of  $\geq 1$  M were used.

**Effect of NaCl on the  $pK_a$  Value for Ionization of the N(3)-H Locus of FAD in FprA.** The pH dependence of the UV-visible absorbance spectrum of oxidized FprA in the presence of 2.5 M NaCl was determined as described in Experimental Procedures. When the pH was increased from 6 to 12, there was a decrease of absorbance at 450 nm, a loss of the well-defined shoulder at  $\sim 475$  nm, and a hypsochromic shift of the flavin peak from 386 to 370 nm (Figure 4A), consistent with deprotonation of the N(3) atom of the flavin cofactor at high pH values (25, 26). A plot of the intensity of the signal at 386 as a function of pH yielded a  $pK_a$  value of  $9.7 \pm 0.02$  (Figure 4A). A control experiment in which the pH titration of oxidized FprA was carried out in the absence of NaCl yielded a  $pK_a$  value of  $10.7 \pm 0.02$  (Figure 4B), consistent with a significant effect of salt on the  $pK_a$  value for the N(3) atom of FAD.

<sup>4</sup> Reduction of the enzyme-bound flavin of FprA at pH 10 in the absence of NaCl started approximately 50 ms after the enzyme was mixed with NADPH, as shown in Figure S2 of the Supporting Information. A possible explanation for such an apparent "lag phase" is that a spectrally silent step occurs in the enzyme-substrate complex prior to the hydride transfer reaction, as kindly suggested by one of the reviewers. Such a spectrally silent step possibly reflects an isomerization of the Michaelis complex occurring at pH 10 to form the catalytically competent species required for the hydride transfer reaction. Since the main goal of the experiment reported here was to evaluate the kinetic behavior of FprA at pH 10 with regard to the CT1 species and determine the dependence of the  $k_{obs}$  values for flavin reduction on NADPH concentration, the apparent lag phase was not investigated further in this study.

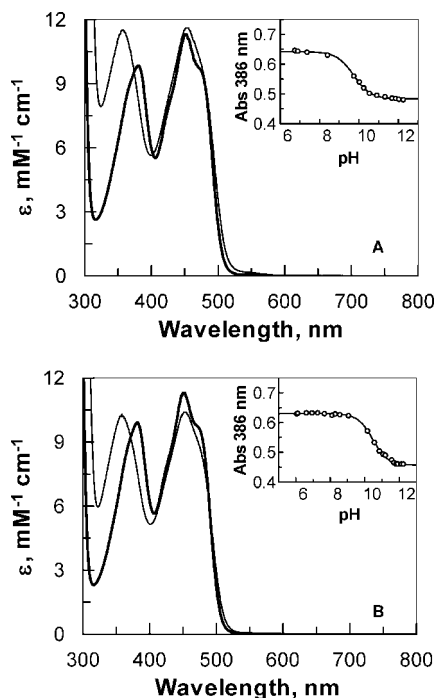
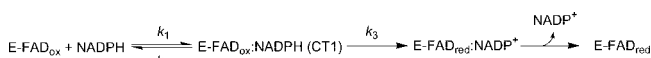


FIGURE 4: Effect of NaCl on the spectral properties of FprA. UV-visible absorbance spectra were recorded in 20 mM sodium phosphate, 20 mM sodium pyrophosphate, and 10% glycerol at 15 °C. (A) FprA in the presence of 2.5 M NaCl; panel B, FprA in the absence of NaCl. Only the spectra of the enzyme at pH 6 (thick solid line) and pH 12 (thin solid line) are shown. The insets show the absorbance value at 386 nm as a function of pH. Data were fit to eq 5.

Scheme 3: Minimal Kinetic Mechanism for the Reductive Half-Reaction of FprA with NADPH in the Presence of  $\geq 1$  M NaCl<sup>a</sup>



<sup>a</sup> E-FAD<sub>ox</sub> and E-FAD<sub>red</sub> represent oxidized and reduced FprA, respectively.

## DISCUSSION

In the presence of NaCl at concentrations that are equal to or greater than 1 M, the anaerobic reduction of FprA with NADPH is consistent with a minimal kinetic mechanism in which formation of the CT1 species is detectable using a stopped-flow spectrophotometer, and the reaction of hydride ion transfer from NADPH to the enzyme-bound flavin appears to be irreversible due to the rapid release of the product (Scheme 3). Evidence supporting this conclusion comes from the lack of an observable CT2 species between the reduced enzyme and the oxidized pyridine nucleotide. This result is indeed readily explained with NADP<sup>+</sup> rapidly dissociating from the reduced enzyme that is formed in the reaction, yielding a negligible concentration of the reduced enzyme–NADP<sup>+</sup> complex that is required for the reverse of the reaction to occur at an appreciable rate. Consistent with the hydride transfer reaction being irreversible, the anaerobic reduction of FprA by NADPH in the presence of  $\geq 1$  M NaCl yielded observed rates for the reduction of the flavin that increased to limiting values with increasing concentrations of substrate, in contrast to what is observed at low ionic strengths (12). Thus, by operating in the presence of  $\geq 1$  M NaCl, we were able for the first time to observe

the formation of the CT1 species between oxidized FprA and NADPH and to simplify the complex kinetic behavior of the enzyme with NADPH as the donor of the hydride ion, thereby rendering the first steps of physiological reaction from NADPH to the enzyme-bound flavin amenable to being studied in detail by stopped-flow techniques. In turn, this allows estimation of all three rate constants of the mechanism shown in Scheme 3, as outlined below. Since the *C* values (eq 3) determined from the plots of the NADPH concentration dependencies of the *k*<sub>obs1</sub> values at various concentrations of salt at pH 7 were in the same range as the *k*<sub>lim</sub> values (eq 4) determined in plots of *k*<sub>obs2</sub> as a function of NADPH concentration (Table 1), the kinetic data could not be analyzed by assuming a rapid equilibrium of NADPH and FprA, for which *k*<sub>2</sub> must be significantly larger than *k*<sub>3</sub> (24). This, in turn, establishes that the *C* values are not simply given by the *k*<sub>2</sub> values, but instead, they must include the kinetic rate constants that account for the second step of the reaction in which the hydride ion is transferred to the flavin, where *C* = *k*<sub>2</sub> + *k*<sub>lim</sub> (24). The results of this analysis are summarized in Table 1.

The rate for the reaction of hydride ion transfer catalyzed by FprA is not affected by the presence or absence of the phosphate group on the pyridine nucleotide that acts as a hydride donor to the flavin, as suggested by the kinetic data with NADPH and NADH presented in this study and previous studies (12). Indeed, since the reaction of hydride transfer to the flavin with NADPH is irreversible (see above), the limiting value for the anaerobic flavin reduction of 18.5 s<sup>−1</sup> determined in this study at saturating concentrations of NADPH (*k*<sub>lim</sub>) in the presence of 1 M NaCl and pH 7 is a good approximation of the rate constant *k*<sub>3</sub> for the chemical step of hydride transfer in FprA (Scheme 3). This value compares well with those recently reported for the reactions of FprA at pH 7 with NADH or NADPH in the presence of 0.1 M NaCl, with values of  $\sim 18$  s<sup>−1</sup> (12). These kinetic data also suggest that moderate concentrations of salt in the reaction mixture have little effect on the chemical step of hydride transfer, implying that the interaction between the nicotinamide and the isalloxazine moieties within the enzyme–substrate complex remains essentially unchanged when the salt concentration of the medium is increased to 1 M. In agreement with this conclusion, an independent study previously showed that the enzymatic activity of FprA remains unchanged in the presence of up to 1 M NaCl (27). Similarly, increasing the pH by 3 units had very little effect on the hydride transfer rate: the *k*<sub>3</sub> values determined at pH 7 and 10 in the presence of 2.5 M NaCl were 10.2 and 9.2 s<sup>−1</sup>, respectively. In contrast, when the NaCl concentration was increased from 1 to 2.5 M at pH 7, an  $\sim 40\%$  decrease in *k*<sub>3</sub> resulted. While the latter observation was not investigated further here, we speculate that such a decrease in the rate of the chemical step may be due to FprA having a slightly different conformation and catalytic behavior in high salt with respect to low- or moderate-salt environments. In this respect, recent biophysical studies demonstrated that the modulation of intramolecular ionic interactions, which are necessarily sensitive to the concentration of salt in the environment, induce significant conformational changes in FprA (27).

It is of interest to evaluate the role of the 2'-phosphate group of the dinucleotide in the association and dissociation

of the FprA–substrate complex. A value of  $140 \text{ mM}^{-1} \text{ s}^{-1}$  has recently been reported for the rate constant of the NADH association to form a CT1 species with FprA at  $25^\circ\text{C}$ , pH 7, and 0.1 M NaCl (12). Here we show that the same process occurred with NADPH with a rate constant that was twice as high as that with NADH under the same conditions, but in the presence of 1 M NaCl (Table 1). The second-order rate constant for the association ( $k_1$ ) of NADPH and FprA to yield a CT1 species at pH 7 is inversely and linearly dependent on the NaCl concentration within the concentration range considered (Figure S4 of the Supporting Information).<sup>5</sup> Although it is inappropriate to assume that such linearity extends below 1 M NaCl, it is expected that  $k_1$  at 0.1 M NaCl would be much higher than  $\sim 300 \text{ mM}^{-1} \text{ s}^{-1}$ , thus making significant the contribution of 2'-phosphate of NADPH to the formation of the Michaelis complex with FprA.

The first-order rate constant for the dissociation ( $k_2$ ) of the NADPH–FprA complex is poorly dependent on the NaCl concentration in the 1–3 M range, with an average value of approximately  $3 \text{ s}^{-1}$  at  $25^\circ\text{C}$  and pH 7 (Table 1). The small magnitudes of the  $k_2$  values support the notion that the dissociation of the pyridine nucleotide from the oxidized enzyme must involve a change in the conformation of the FprA–NADPH complex that limits the rate of dissociation of NADPH from the active site of the enzyme. In this context, the comparison of the ligand-free and NADP(H)-bound crystal forms of the analogous enzyme adrenodoxin reductase previously suggested that this enzyme undergoes an induced-fit process upon substrate binding (19). In contrast, the kinetic pattern observed at pH 10 in the presence of a high salt concentration, i.e., 2.5 M, is consistent with NADPH binding to FprA in rapid equilibrium. This, in turn, is consistent with  $k_2$  being significantly larger than  $k_3$  at high pH, suggesting that the conformational change that is associated with the dissociation of the pyridine nucleotide from the enzyme does not limit the overall rate of the dissociation process. Interestingly, a similar analysis of previously reported data shows that the rate constant  $k_2$  for NADH determined at pH 7 is only slightly larger than that determined with NADPH, with a value of  $\sim 6 \text{ s}^{-1}$  (from the data in Figure 5 of ref 12). Thus, there is a minimal effect on the rate constant for the dissociation of the pyridine nucleotide from the active site of the oxidized enzyme that is exerted by the 2'-phosphate group of NADPH.

The CT1 species between FprA and NADPH can be observed only with the oxidized flavin in the neutral state, but not with a negatively charged flavin. Evidence supporting this conclusion comes from the anaerobic reduction of the enzyme with NADPH at high pH in the presence and absence of salt. The pH titration of the UV–visible absorbance spectrum of FprA in the presence of 2.5 M NaCl established a  $\text{p}K_a$  of 9.7 for ionization of the N(3)-H locus of FAD (25). Thus, at the pH value of 10 at which the CT1 species was not observed in the stopped-flow experiments, approximately two-thirds of the oxidized flavin is present in the anionic

state. In contrast, at high pH and in the absence of salt, conditions under which the CT1 species was observed within the dead time of the mixing of FprA with NADPH, the  $\text{p}K_a$  for the ionization of the N(3) atom of the flavin was 10.7, consistent with approximately 85% of the flavin being in the neutral state. The lack of formation of a CT1 species when the oxidized flavin is anionic is readily explained by considering that in the charge transfer process NADPH acts as the charge donor and the flavin acts as the charge acceptor, which is required to be electron poor (26, 28, 29). Furthermore, the shift in the  $\text{p}K_a$  value for the ionization of the N(3)-H group of the oxidized flavin observed with an increase in the concentration of salt in solution is likely due to the anionic form of the flavin being favored with respect to the neutral one in the presence of high concentrations of salt in solution.

The rate of transfer of the hydride ion from NADPH to the oxidized flavin is the same irrespective of whether a charge transfer species is observed between the hydride donor and acceptor. This conclusion is supported by the kinetic data in the presence and absence of salt at pH 10, showing similar rate constants for the hydride transfer reaction to the enzyme-bound flavin of  $\sim 10 \text{ s}^{-1}$ , from a CT1 species (i.e., in the absence of NaCl), and from a Michaelis complex showing no charge transfer character (i.e., in the presence of 2.5 M NaCl). We have previously shown that the reaction of hydride ion transfer in FprA is highly sensitive to precise geometry that defines the interaction of the nicotinamide moiety with the isoalloxazine ring of the flavin cofactor in the active site of the enzyme (12). Consequently, it is strongly suggested that both pH and salt conditions that suppress the charge transfer character of this interaction do not affect the relative orientation and distance between the nicotinamide and isoalloxazine rings within the enzyme–substrate complex. The mechanistic implication of this observation is that the formation of a charge transfer between a charge donor and a charge acceptor is not required for and does not favor the efficient transfer of the charge from a donor species to an acceptor species as a hydride ion.

In conclusion, by studying the reductive half-reaction of FprA with NADPH using rapid kinetic techniques in the presence of high concentrations of salt or high pH, we have dissected the enzymatic reaction in its elementary kinetic steps. This approach has allowed the first direct observation of the formation of the initial Michaelis complex, i.e., the CT1 species, between FprA and NADPH, and an unambiguous determination of the second-order rate constants for its formation with NADPH as the substrate. Furthermore, all the kinetic rate constants associated with the reductive half-reaction of the enzyme with NADPH have been determined, allowing for a direct comparison with those previously determined with NADH. The kinetic data presented in this study represent a firm framework for the interpretation of future studies on the interaction of adrenodoxin-like enzymes with NADPH. Furthermore, due to the similarity displayed by the kinetic mechanisms of mitochondrial and plastidial subtypes of ferredoxin reductases (2, 30, 31), the experimental approach presented herein is expected to be helpful also in the study of other NADPH-dependent plant-type ferredoxin-NADP<sup>+</sup> reductases, as well as medically relevant enzymes such as cytochrome P450 reductase, nitric oxide synthase, and adrenodoxin reductase.

<sup>5</sup> In principle, the dependence of the  $k_1$  value on NaCl concentration may be due to an effect of the ionic strength, the specific ions ( $\text{Na}^+$  or  $\text{Cl}^-$ ), or the viscosity of the solvent. Since these contributions were not investigated further in this study, we opted to use the concentration of salt rather than either ionic strength or solvent viscosity in our analysis.

## SUPPORTING INFORMATION AVAILABLE

Figure S1 shows the dependence of the observed rates of reduction of FprA in the presence of 2 and 2.5 M NaCl on the concentration of NADPH at pH 7. Figure S2 shows stopped-flow traces at 530 nm acquired at pH 10 for the anaerobic reduction of FprA with NADPH. Figure S3 shows the dependence of the observed rates ( $k_{\text{obs}}$ ) for flavin reduction determined at 450 nm on the concentration of NADPH at pH 10. Figure S4 shows the dependence of the  $k_1$  values for the formation of the CT1 species between FprA and NADPH on the concentration of NADPH at pH 7. This material is available free of charge via the Internet at <http://pubs.acs.org>.

## REFERENCES

- Hurley, J. K., Morales, R., Martinez-Julvez, M., Brodie, T. B., Medina, M., Gomez-Moreno, C., and Tollin, G. (2002) Structure-function relationships in *Anabaena* ferredoxin/ferredoxin:NADP<sup>+</sup> reductase electron transfer: Insights from site-directed mutagenesis, transient absorption spectroscopy and X-ray crystallography. *Biochim. Biophys. Acta* 1554, 5–21.
- Batie, C. J., and Kamin, H. (1986) Association of ferredoxin-NADP<sup>+</sup> reductase with NADP(H) specificity and oxidation-reduction properties. *J. Biol. Chem.* 261, 11214–11223.
- Aliverti, A., Piubelli, L., Zanetti, G., Lubberstedt, T., Herrmann, R. G., and Curti, B. (1993) The role of cysteine residues of spinach ferredoxin-NADP<sup>+</sup> reductase as assessed by site-directed mutagenesis. *Biochemistry* 32, 6374–6380.
- Nogues, I., Perez-Dorado, I., Frago, S., Bittel, C., Mayhew, S. G., Gomez-Moreno, C., Hermoso, J. A., Medina, M., Cortez, N., and Carrillo, N. (2005) The ferredoxin-NADP(H) reductase from *Rhodobacter capsulatus*: Molecular structure and catalytic mechanism. *Biochemistry* 44, 11730–11740.
- Sugiyama, T., Miura, R., and Yamano, T. (1979) Differences between the reactivities of two pyridine nucleotides in the rapid reduction process and the reoxidation process of adrenodoxin reductase. *J. Biochem.* 86, 213–223.
- Light, D. R., and Walsh, C. (1980) Flavin analogs as mechanistic probes of adrenodoxin reductase-dependent electron transfer to the cholesterol side chain cleavage cytochrome P-450 of the adrenal cortex. *J. Biol. Chem.* 255, 4264–4277.
- Gutierrez, A., Lian, L. Y., Wolf, C. R., Scrutton, N. S., and Roberts, G. C. (2001) Stopped-flow kinetic studies of flavin reduction in human cytochrome P450 reductase and its component domains. *Biochemistry* 40, 1964–1975.
- Gutierrez, A., Grunau, A., Paine, M., Munro, A. W., Wolf, C. R., Roberts, G. C., and Scrutton, N. S. (2003) Electron transfer in human cytochrome P450 reductase. *Biochem. Soc. Trans.* 31, 497–501.
- Knight, K., and Scrutton, N. S. (2002) Stopped-flow kinetic studies of electron transfer in the reductase domain of neuronal nitric oxide synthase: Re-evaluation of the kinetic mechanism reveals new enzyme intermediates and variation with cytochrome P450 reductase. *Biochem. J.* 367, 19–30.
- Daff, S. (2004) An appraisal of multiple NADPH binding-site models proposed for cytochrome P450 reductase, NO synthase, and related diflavin reductase systems. *Biochemistry* 43, 3929–3932.
- McLean, K. J., Scrutton, N. S., and Munro, A. W. (2003) Kinetic, spectroscopic and thermodynamic characterization of the *Mycobacterium tuberculosis* adrenodoxin reductase homologue FprA. *Biochem. J.* 372, 317–327.
- Pennati, A., Razeto, A., de Rosa, M., Pandini, V., Vanoni, M. A., Mattevi, A., Coda, A., Aliverti, A., and Zanetti, G. (2006) Role of the His57-Glu214 ionic couple located in the active site of *Mycobacterium tuberculosis* FprA. *Biochemistry* 45, 8712–8720.
- Fischer, F., Raimondi, D., Aliverti, A., and Zanetti, G. (2002) *Mycobacterium tuberculosis* FprA, a novel bacterial NADPH-ferredoxin reductase. *Eur. J. Biochem.* 269, 3005–3013.
- Bossi, R. T., Aliverti, A., Raimondi, D., Fischer, F., Zanetti, G., Ferrari, D., Tahallah, N., Maier, C. S., Heck, A. J., Rizzi, M., and Mattevi, A. (2002) A covalent modification of NADP<sup>+</sup> revealed by the atomic resolution structure of FprA, a *Mycobacterium tuberculosis* oxidoreductase. *Biochemistry* 41, 8807–8818.
- Omura, T., Sato, R., Cooper, D. Y., Rosenthal, O., and Estabrook, R. W. (1965) Function of cytochrome P-450 of microsomes. *Fed. Proc.* 24, 1181–1189.
- Lambeth, J. D., Geren, L. M., and Millett, F. (1984) Adrenodoxin interaction with adrenodoxin reductase and cytochrome P-450<sub>sc</sub>. Cross-linking of protein complexes and effects of adrenodoxin modification by 1-ethyl-3-(3-dimethylaminopropyl)carbodiimide. *J. Biol. Chem.* 259, 10025–10029.
- Cole, S. T., and Barrell, B. G. (1998) Analysis of the genome of *Mycobacterium tuberculosis* H37Rv. *Novartis Found. Symp.* 217, 160–177.
- McLean, K. J., Warman, A. J., Seward, H. E., Marshall, K. R., Girvan, H. M., Cheesman, M. R., Waterman, M. R., and Munro, A. W. (2006) Biophysical characterization of the sterol demethylase P450 from *Mycobacterium tuberculosis*, its cognate ferredoxin, and their interactions. *Biochemistry* 45, 8427–8443.
- Ziegler, G. A., Vonnrhein, C., Hanukoglu, I., and Schulz, G. E. (1999) The structure of adrenodoxin reductase of mitochondrial P450 systems: Electron transfer for steroid biosynthesis. *J. Mol. Biol.* 289, 981–990.
- Ziegler, G. A., and Schulz, G. E. (2000) Crystal structures of adrenodoxin reductase in complex with NADP<sup>+</sup> and NADPH suggesting a mechanism for the electron transfer of an enzyme family. *Biochemistry* 39, 10986–10995.
- de Rosa, M., Pennati, A., Pandini, V., Monzani, E., Zanetti, G., and Aliverti, A. (2007) Enzymatic oxidation of NADP<sup>+</sup> to its 4-oxo derivative is a side-reaction displayed only by the adrenodoxin reductase type of ferredoxin-NADP<sup>+</sup> reductases. *FEBS J.* 274, 3998–4007.
- Kamerbeek, N. M., Fraaije, M. W., and Janssen, D. B. (2004) Identifying determinants of NADPH specificity in Baeyer-Villiger monooxygenases. *Eur. J. Biochem.* 271, 2107–2116.
- Levy, H. R., Vought, V. E., Yin, X., and Adams, M. J. (1996) Identification of an arginine residue in the dual coenzyme-specific glucose-6-phosphate dehydrogenase from *Leuconostoc mesenteroides* that plays a key role in binding NADP<sup>+</sup> but not NAD<sup>+</sup>. *Arch. Biochem. Biophys.* 326, 145–151.
- Strickland, S., Palmer, G., and Massey, V. (1975) Determination of dissociation constants and specific rate constants of enzyme-substrate (or protein-ligand) interactions from rapid reaction kinetic data. *J. Biol. Chem.* 250, 4048–4052.
- Ghanem, M., and Gadda, G. (2005) On the catalytic role of the conserved active site residue His466 of choline oxidase. *Biochemistry* 44, 893–904.
- De Colibus, L., and Mattevi, A. (2006) New frontiers in structural flavoenzymology. *Curr. Opin. Struct. Biol.* 16, 722–728.
- Bhatt, A. N., Shukla, N., Aliverti, A., Zanetti, G., and Bhakuni, V. (2005) Modulation of cooperativity in *Mycobacterium tuberculosis* NADPH-ferredoxin reductase: Cation- and pH-induced alterations in native conformation and destabilization of the NADP<sup>+</sup>-binding domain. *Protein Sci.* 14, 980–992.
- Massey, V., and Palmer, G. (1962) Charge transfer complexes of lipoyl dehydrogenase and free flavins. *J. Biol. Chem.* 237, 2347–2358.
- Scarborough, F. E., Shieh, H., and Voet, D. (1976) Crystal structure of a complex between lumiflavin and 2,6-diamino-9-ethylpurine: A flavin adenine dinucleotide model exhibiting charge-transfer interactions. *Proc. Natl. Acad. Sci. U.S.A.* 73, 3807–3811.
- Tejero, J., Peregrina, J. R., Martinez-Julvez, M., Gutierrez, A., Gomez-Moreno, C., Scrutton, N. S., and Medina, M. (2007) Catalytic mechanism of hydride transfer between NADP<sup>+</sup>/H and ferredoxin-NADP<sup>+</sup> reductase from *Anabaena* PCC 7119. *Arch. Biochem. Biophys.* 459, 79–90.
- Aliverti, A., Bruns, C. M., Pandini, V. E., Karplus, P. A., Vanoni, M. A., Curti, B., and Zanetti, G. (1995) Involvement of serine 96 in the catalytic mechanism of ferredoxin-NADP<sup>+</sup> reductase: Structure–function relationship as studied by site-directed mutagenesis and X-ray crystallography. *Biochemistry* 34, 8371–8379.

BI702250H